JACC: BASIC TO TRANSLATIONAL SCIENCE VOL. 6, NO. 12, 2021

PRECLINICAL RESEARCH

Abnormal Flow Conditions Promote Endocardial Fibroelastosis Via Endothelial-to-Mesenchymal Transition, Which Is Responsive to Losartan Treatment

Nicholas A. Oh, MD,[a,b] Xuechong Hong, MD, PhD,[a] Ilias P. Doulamis, MD, PhD,[a] Elamaran Meibalan, PhD,[c] Teresa Peiseler, MD,[a] Juan Melero-Martin, PhD,[a] Guillermo García-Cardeña, PhD,[c] Pedro J. del Nido, MD,[a] Ingeborg Friehs, MD[a]

VISUAL ABSTRACT

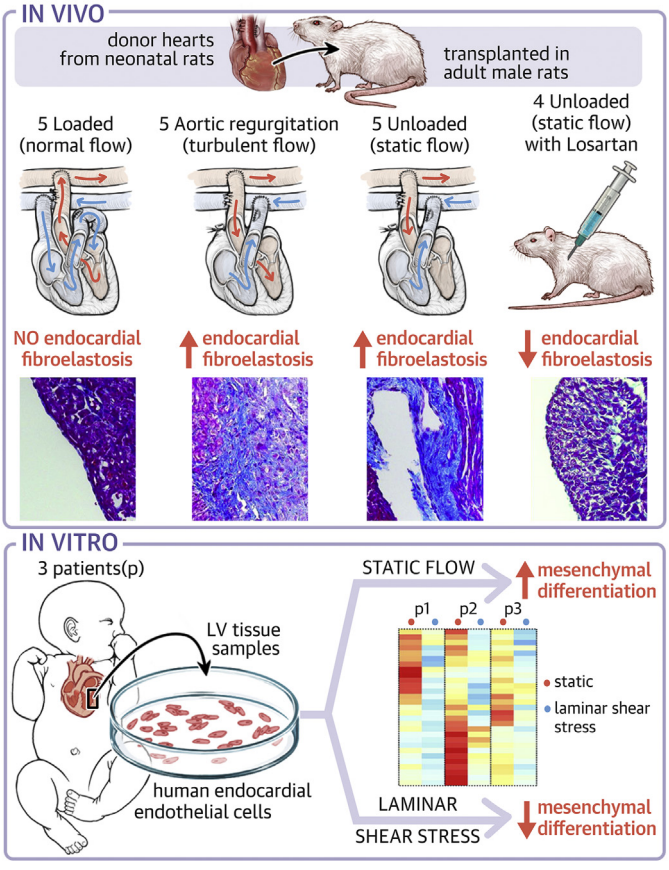

Oh, N.A. et al. J Am Coll Cardiol Basic Trans Science. 2021;6(12):984–999.

HIGHLIGHTS

- **EFE is a congenital cardiac pathology contributing to increased morbidity and mortality. The pathologic triggers of EFE remain to be characterized.**
- **To determine whether abnormal flow promotes EFE development, we used in vivo neonatal rodent surgical models and an in vitro model using human primary endocardial cells**
- **We established novel surgical model with flow profiles seen in patients that develop EFE. Static and turbulent flow conditions promoted EFE development in neonatal rodent hearts.**
- **Losartan treatment is shown to significantly ameliorate EFE progression and decreases mRNA and protein expression of EndoMT markers in neonatal rodent hearts.**
- **RNAseq analysis of human endocardial cells subjected to different flow conditions show that normal flow suppresses gene expression critical for mesenchymal differentiation and Notch signaling.**

From the [a]Department of Cardiac Surgery, Boston Children's Hospital, Boston, Massachusetts, USA; [b]Department of Cardiothoracic Surgery, Cleveland Clinic Foundation, Cleveland, Ohio, USA; and the [c]Laboratory for Systems Mechanobiology, Center for Excellence in Vascular Biology, Department of Pathology, Brigham and Women's Hospital, Boston, Massachusetts, USA.

ISSN 2452-302X https://doi.org/10.1016/j.jacbts.2021.10.002

SUMMARY

Endocardial fibroelastosis (EFE) is defined by fibrotic tissue on the endocardium and forms partly through aberrant endothelial-to-mesenchymal transition. However, the pathologic triggers are still unknown. In this study, we showed that abnormal flow induces EFE partly through endothelial-to-mesenchymal transition in a rodent model, and that losartan can abrogate EFE development. Furthermore, we translated our findings to human endocardial endothelial cells, and showed that laminar flow promotes the suppression of genes associated with mesenchymal differentiation. These findings emphasize the role of flow in promoting EFE in endocardial endothelial cells and provide a novel potential therapy to treat this highly morbid condition.

ABBREVIATIONS AND ACRONYMS

α-SMA = alpha-smooth muscle actin

AR = aortic regurgitation

EFE = endocardial fibroelastosis

EndoMT = endothelial-to-mesenchymal transition

GO = gene ontology

HLHS = hypoplastic left heart syndrome

HUEEC = human endocardial endothelial cells

HUVEC = human umbilical vein endothelial cells

LSS = laminar shear stress

LV = left ventricle

Endocardial fibroelastosis (EFE) is a cardiac pathology found in certain congenital heart defects and is defined by de novo endocardial fibrosis that encapsulates the myocardium. Typically, EFE is found in the left ventricle (LV) and can extend into the left atrium and pulmonary veins (1). The presence of this fibroelastic scar-like tissue on the endocardium causes severe restriction of diastolic compliance, leading to systolic and diastolic dysfunction and ultimately heart failure. The severity of EFE can vary from patient to patient, but multiple studies have shown that the presence of EFE leads to higher morbidity and mortality (2-5). This is particularly apparent in patients with hypoplastic left heart syndrome (HLHS), a disease defined by a spectrum of left heart-aorta complex underdevelopment, consisting of atresia, stenosis, or hypoplasia of the aortic and/or mitral valve with marked hypoplasia of the LV (2,3). Although surgical and catheter therapies for HLHS (such as biventricular repair and fetal aortic valvuloplasty) are continuing to evolve, the lack of effective drugs for EFE limits the effectiveness of these treatments (4,5).

The mechanism by which EFE is formed is hypothesized to be, at least in part, through aberrant endothelial-to-mesenchymal transition (EndoMT) of the endocardium (6). Multiple studies have suggested that endocardial cells, a specialized type of endothelial cells, are triggered to undergo EndoMT towards a mesenchymal phenotype through various pathways such as the transforming growth factor (TGF)-β and Notch signaling pathways (6-8). Histologic data show that EndoMT occurs at the subendocardial layer of human EFE tissue (6,9). Lately, lineage tracing studies indicate epicardial-to-mesenchymal transition as alternative underlying mechanism for EFE (10). The mechanism of EFE development is further complicated by the role of flow dynamics, genetics, epigenetics, and/or inflammation as potential inciters of EFE (11-14). Thus, it is critical to understand the mechanism of EFE development in the context of these other factors. Interestingly, clinical observations have reported an association between increased EFE formation and flow disturbances within the LV from mitral and/or aortic valve dysfunction (9). Previous studies provide ample evidence of the differential response that the vascular endothelium displays in response to distinct types of flow (15,16). Specifically, human umbilical vein endothelial cells (HUVECs) and bovine aortic endothelial cells display a dysfunctional phenotype when exposed to disturbed flow (17,18). Furthermore, evidence suggests that atherosclerosis in the carotid arteries involves EndoMT that is triggered by abnormal, disturbed flow at the bifurcation (19). Although evidence for flow-mediated EndoMT in vascular endothelium is well documented, no research has been performed on abnormal flow and its effect on endocardium. This study sought to understand these effects on neonatal endocardial endothelial cells by using an in vivo animal model that can simulate flow conditions often seen in patients who develop EFE. Additionally, we sought to show the effects of flow by exposing human

The authors attest they are in compliance with human studies committees and animal welfare regulations of the authors' institutions and Food and Drug Administration guidelines, including patient consent where appropriate. For more information, visit the Author Center.

Manuscript received January 20, 2021; revised manuscript received October 5, 2021, accepted October 5, 2021.

JACC: BASIC TO TRANSLATIONAL SCIENCE VOL. 6, NO. 12, 2021
DECEMBER 2021:984–999

endocardial endothelial cells (HUEECs) isolated from normal LV tissue to define stress, which has not been previously described. We then used losartan (a clinically relevant and widely available drug shown to decrease TGF-β production) as a potential therapy to block EndoMT and curb EFE development.

METHODS

A detailed Methods section is available in the Supplemental Appendix (including Supplemental Tables 1 to 4).

NEONATAL RODENT HETEROTOPIC HEART TRANSPLANTATION. Heterotopic heart transplantation was performed in Lewis rats using techniques previously described (20,21). In brief, donor hearts were obtained from neonatal rats (2 to 4 days of age) and were transplanted in young adult male rats (weighing 100 to 120 g) (n = 5 per group). The donor animal received 300 IU heparin and the heart was explanted through a midline thoracic incision followed by storage in cold high-potassium Krebs-Henseleit solution, as previously described. The recipient animal was anesthetized with ketamine (40 to 60 mg/kg intraperitoneally), xylazine (10 mg/kg intraperitoneally), and isoflurane via endotracheal tube. In the unloaded/static flow model, the heart was implanted in the infrarenal position, taking care to anastomose the donor aorta to recipient abdominal aorta, and donor pulmonary artery to recipient inferior vena cava. In the aortic regurgitation/regurgitant flow model, the donor aortic valve was disrupted using a sterile spiral guidewire (0.525-mm diameter), and the donor heart was implanted in a similar fashion to the unloaded model. In the loaded/normal flow model, the donor PA was anastomosed to the donor left atrial appendage before transplantation. The donor heart was then transplanted in the infrarenal position, taking care to anastomose the donor aorta with recipient abdominal aorta, and donor superior vena cava with the recipient inferior vena cava. Analgesia was provided to the recipient animal using buprenorphine sustained release (0.1 to 0.5 mg/kg subcutaneously) immediately postoperatively and meloxicam (1 mg/kg subcutaneously) every 24 hours for 3 days, as needed. In the losartan (Aurobindo Pharma, Hyderabad, India) treatment group, the donor heart was transplanted in a similar fashion to the static flow hearts and losartan was administered (40 mg/kg/day) intraperitoneally throughout the duration of the study. For the native, loaded, unloaded, and aortic regurgitation groups, we used 5 animals per group. For the losartan treatment and vehicle treatment groups, we used 4 animals per group. Animals were survived for 1 week and were euthanized with inhaled carbon dioxide and exsanguination through excision of the transplanted heart and native heart.

HUMAN LV ENDOCARDIAL TISSUE. Human endocardial tissue from the LV was collected in accordance with an Institutional Review Board–approved protocol IRB-P00006097. Tissues included in this study were from patients who underwent cardiac surgery at Boston Children's Hospital, required resection of endocardial tissue, and did not have any valvular abnormalities or a hypoplastic left ventricle. Resected tissues that were determined to be discarded were instead used for this study. A total of 3 patient samples were used, and their characteristics can be found in Supplemental Table 1.

ISOLATION AND CULTURE OF HUMAN ENDOCARDIAL ENDOTHELIAL CELLS. Once discarded human endocardial tissue was obtained from the operating suite, the tissue was placed in normal saline solution. Sterile instruments were used to carefully resect any underlying myocardium off of the endocardial layer. This endocardial layer was then minced and digested using collagenase A, collagenase II, and dispase. After 1.5 to 2 hours of digestion at 37°C with gentle shaking, the reaction was quenched using D10 solution, and anti-hu-CD31 Dynabeads CD31 (ThermoFisher, Cat. No. 1115D) were used to positively select CD31+ endocardial endothelial cells. CD31+ cells were plated on 1% gelatin-coated plates and cultured in endothelial cell growth medium (EGM)-2 (PromoCell, Cat. No. C-22010). EGM-2 Medium was changed every 2 days. HUEEC colonies with spindle-like cell morphology emerged in culture after 3 to 4 days. HUEECs were then cultured on 1% gelatin-coated plates using EGM-2 medium. All experiments were performed with HUEECs before passage 8.

WALL SHEAR STRESS/FLOW EXPERIMENTS. HUEECs were exposed to laminar shear stress using a dynamic flow system (DFS). DFS is a multicomponent cone and plate viscometer that provides a controlled culture environment for a cell monolayer and can apply a specified wall shear stress, as described in previous work (15). In brief, isolated HUEECs were plated at a density of 70,000 cells/cm^2 onto a custom designed 10.8-cm diameter polystyrene plate surface (Plaskolite, Inc.). A confluent monolayer was maintained for 48 hours in EGM-2 medium at 37 °C. Before the start of the flow experiments, the plate was washed using cold phosphate-buffered saline solution, and incubated in EGM-2 media again. The custom plate was then positioned onto the base of the microscope stage, and the cone was lowered into position

at the center of the plate. The HUEECs were maintained under static (no flow conditions) or exposed to uniform laminar shear stress (LSS) (5 dynes/cm^2). EGM-2 media was exchanged through the side ports at a rate of 0.07 cc/min. The cells were subjected to LSS for 24 hours before harvesting for following analyses.

RNA SEQUENCING ANALYSIS. RNA sequencing (RNAseq) was performed on 3 sets of samples. Each set had HUEECs isolated from 1 specific patient and subjected to the 2 different wall shear stresses (static and 5 dyne/cm^2 uniform LSS) (6 specimens). Cell pellets were isolated after the 24-hour flow experiment and was frozen using liquid nitrogen. Samples were sent to GENEWIZ overnight and were processed by GENEWIZ facilities. RNA quantity and quality were inspected, and libraries were prepared and sequenced by GENEWIZ. Library preparation involved mRNA enrichment and fragmentation, chemical fragmentation, first- and second-strand cDNA synthesis, end repair and 5' phosphorylation, Da-tailing, adaptor ligation, and polymerase chain reaction (PCR) enrichment. Libraries were then sequenced using Illumina HiSeq2500 platform (Illumina) using 2 × 150 paired end configuration. Raw sequencing data (FASTQ files) were examined for library generation and sequencing using FastQC (Babraham Institute) to ensure data quality. Reads were aligned to University of California Santa Cruz hg38 genome using the STAR aligner. Alignments were checked for evenness of coverage, ribosomal RNA content, genomic context of alignments, complexity, and other quality checks using a combination of FastQC, Qualimap and MultiQC. The expression of the transcripts was quantified against the Ensembl release GRCh38 transcriptome annotation using Salmon. These transcript abundances were then imported into R (version 3.5.1) and aggregated to the gene level with tximport. Differential expression at the gene level was called with DESeq2. Pairwise differential expression analysis between groups was performed using Wald significance test. *P* values were corrected for multiple hypotheses testing with the Benjamini-Hochberg false-discovery rate procedure (adjusted *P* value). Genes with adjusted $P < 0.05$ were considered significantly different. Principal component analyses were performed on DESeq2 normalized, rlog variance stabilized reads. Volcano plots of enriched gene sets were generated with ggplot2 package. The differentially expressed genes were also compared to curated pathway from Kyoto Encyclopedia of Genes and Genomes (KEGG) database using the Gene Set Enrichment Analysis tool. Heat maps of differential expressed genes and enriched gene sets were generated with heatmap package. The RNAseq datasets are deposited online with Sequence Read Archive accession number: PRJNA638937.

STATISTICAL ANALYSES. All statistical analyses were performed using the GraphPad Prism v.5 software (GraphPad Software Inc). Unless otherwise stated, data are expressed as mean ± SD. Comparisons between multiple groups were performed by analysis of variance followed by Benjamin Hochberg's false-discovery rate post hoc analysis. Unpaired 2-tailed Student *t* tests were used for comparisons between 2 groups. Sample size, including number of mice per group, was chosen to ensure adequate power (80%) and were based on historical laboratory data. No exclusion criteria were applied for any analyses, and $P < 0.05$ was considered to be statistically significant.

DATA AVAILABILITY. The authors declare that all data supporting the findings of this study are available in the paper and the Supplemental Appendix.

RESULTS

NEONATAL HETEROTOPIC HEART TRANSPLANTATION WITH DIFFERENT LV FLOW CONDITIONS FOR EFE MODELING. Neonatal heterotopic heart transplantation has been developed as an animal model of EFE formation (20,21). These transplanted hearts undergo EndoMT and subsequent EFE development, presumably from the lack of normal blood flow through the LV. However, detailed investigation on how the absence of normal flow affects EFE development has not been performed. Additionally, the effects of other flow profiles on promoting or abrogating EndoMT and thus EFE formation in the LV endocardium (namely, regurgitant flow and reconstitution of LV flow) has not been studied. This is critical in understanding EFE development in patients with regurgitant flow, and potentially the effects of reconstituting normal flow. Using techniques described previously, 6-day-old neonatal rodent hearts were transplanted into the abdomen of recipient rodent and reperfused with different flow conditions. Through different combinations of arterial and venous anastomoses, various flow profiles in the LV can be achieved, specifically unloaded/static flow (n = 5), aortic regurgitation (AR) /regurgitant flow (n = 5), and loaded/normal flow (n = 5) (**Figure 1A**).

At 7 days post-transplantation, echocardiography confirmed flow patterns in the hearts: the static group with severely limited flow in the LV, the AR/regurgitant flow group had a regurgitant jet (moderate to severe AR) into the LV, and the normal

FIGURE 1 **Neonatal Heterotopic Heart Transplantation With Different Left Ventricular Flow Conditions for EFE Modeling**

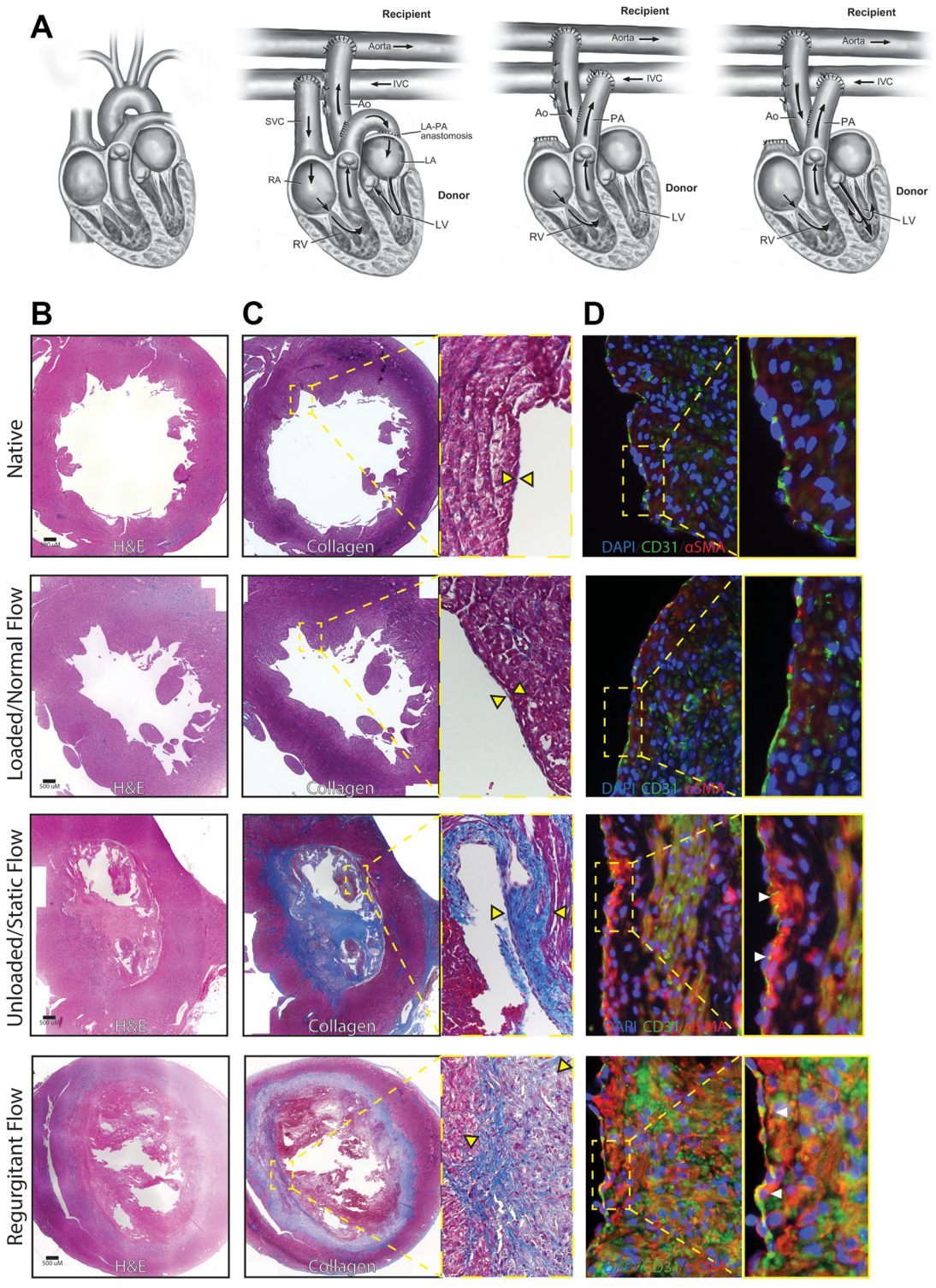

Continued on the next page

flow group had flow through the LV and out of the aorta. Animals were included in their respective group once verified by echocardiography. Using an established graft beating score (0 to 4) where a score of 4 describes normal beating and amplitude and 0 describes nonbeating, we observed the AR/regurgitant flow group contracted significantly less vigorously thus had a lower score, whereas the other groups continued to contract well (Supplemental Figure 1A). On gross observation of the transplanted heart, the static and AR/regurgitant flow groups had increased LV thickening at the endocardial layer (Supplemental Figure 1B). The above results show that different flow conditions are established in our heterotopic heart transplantation model, and that the absence of normal flow (namely, static flow and regurgitant flow) develops endocardial thickening similar to EFE.

ABSENCE OF NORMAL BLOOD FLOW IS ASSOCIATED WITH EFE PARTLY THROUGH EndoMT IN ENDOCARDIUM. Once the desired flow profiles were confirmed in each transplanted heart by echocardiography, we evaluated the samples by histology on day 7 post-transplantation. The static group showed increased fibrosis and collagen deposition in the endocardial and subendocardial layers of the LV compared to the in situ native heart, as evidenced by hematoxylin and eosin and Masson trichrome staining. The regurgitant flow group also showed similar levels of fibrosis and collagen deposition as the static group. In contrast, the normal flow group with corrected flow conditions showed little to no fibrosis and collagen deposition, which was histologically similar to the native heart (**Figures 1B and 1C**). The area of fibrosis, which is determined by the area of collagen deposition, showed that the static and regurgitant flow groups had a significantly greater fibrotic area when compared to both the normal flow group and native heart (static vs normal flow: 1.51 ± 0.15 mm^2 vs 0.42 ± 0.13 mm^2, $P = 0.004$; regurgitant vs normal flow: 1.64 ± 0.20 mm^2 vs 0.42 ± 0.13 mm^2, $P = 0.002$) (**Figure 2A**).

A hallmark feature of EFE through EndoMT is an upregulation of mesenchymal markers and down-regulation of endothelial markers, often coexpressing both during this process (22). Histology from surgically resected EFE in patients showed fibrotic tissue within the endocardium, with evidence of EndoMT occurring throughout the specimen (**Figure 2B**). To determine whether the fibrosis identified in our animal model was associated with EndoMT, we evaluated for the endothelial marker, CD31, and mesenchymal marker, alpha-smooth muscle actin (α-SMA), using immunofluorescent staining. The native heart showed CD31 expression in the endocardium and no expression of α-SMA. Similarly, hearts in the normal flow group displayed CD31 and minimal levels of alpha-Smooth Muscle Actin (α-SMA) in the endocardium. However, the endocardium in the static heart group showed coexpression of α-SMA and CD31 at the endocardial border as well as within the thick fibrotic area. Regurgitant flow group hearts also showed coexpression of α-SMA and CD31 at the endocardial border and within the fibrotic area (**Figure 1D**). Collectively, these results showed that different flow conditions induce different levels of EFE formation. More specifically, abnormal blood flow is associated with EndoMT-mediated EFE.

To further validate that EndoMT is responsible for the fibrotic changes caused by the absence of normal flow, we sought evidence at the molecular level by examining the mRNA expression of EndoMT-related markers in the endocardium under the various flow conditions by quantitative PCR (qPCR). mRNA was extracted from dissected endocardial tissue from transplanted neonatal hearts. CD31 expression was not statistically different between the various groups. However, both the static and the regurgitant flow groups had significantly higher mRNA expression of αSMA than native hearts (**Figure 2C**). In contrast, hearts in the normal flow group were found with significantly decreased α-SMA expression when compared to both the static and regurgitant flow group hearts (**Figure 2C**) and had similar α-SMA level

FIGURE 1 Continued

(A) Schema of flow in the left ventricle (LV) after neonatal heterotopic heart transplantation: native heart loaded/normal flow, unloaded/static flow, and regurgitant flow. **(B)** On day 7, native, loaded/normal flow, unloaded/static flow, and regurgitant flow models were examined with hematoxylin and eosin (H&E) staining that demonstrate a large area of fibrosis shown with the unloaded and regurgitant flow models. **(C)** Masson trichrome staining shows increased collagen deposition along the endocardium **(yellow arrowheads)** with the unloaded and regurgitant flow models **(D)** Immunofluorescence staining with 4′,6-diamidino-2-phenylindole (DAPI) **(blue)**, CD31 **(green)**, and αSMA **(red)** shows endocardial endothelial cells in the unloaded and regurgitant flow models undergoing endothelial-to-mesenchymal transition, denoted by co-expression of CD31 and αSMA **(white arrowheads)**, whereas native and loaded models do not. α-SMA = alpha-smooth muscle actin; Ao = aortic; EFE = endocardial fibroelastosis; IVC = inferior vena cava; LA = left atrium; PA = pulmonary artery; RA = right atrium; RV = right ventricle; SVC = superior vena cava.

FIGURE 2 Absence of Normal Blood Flow is Associated With EFE-Like Remodeling Through EndoMT in Endocardium

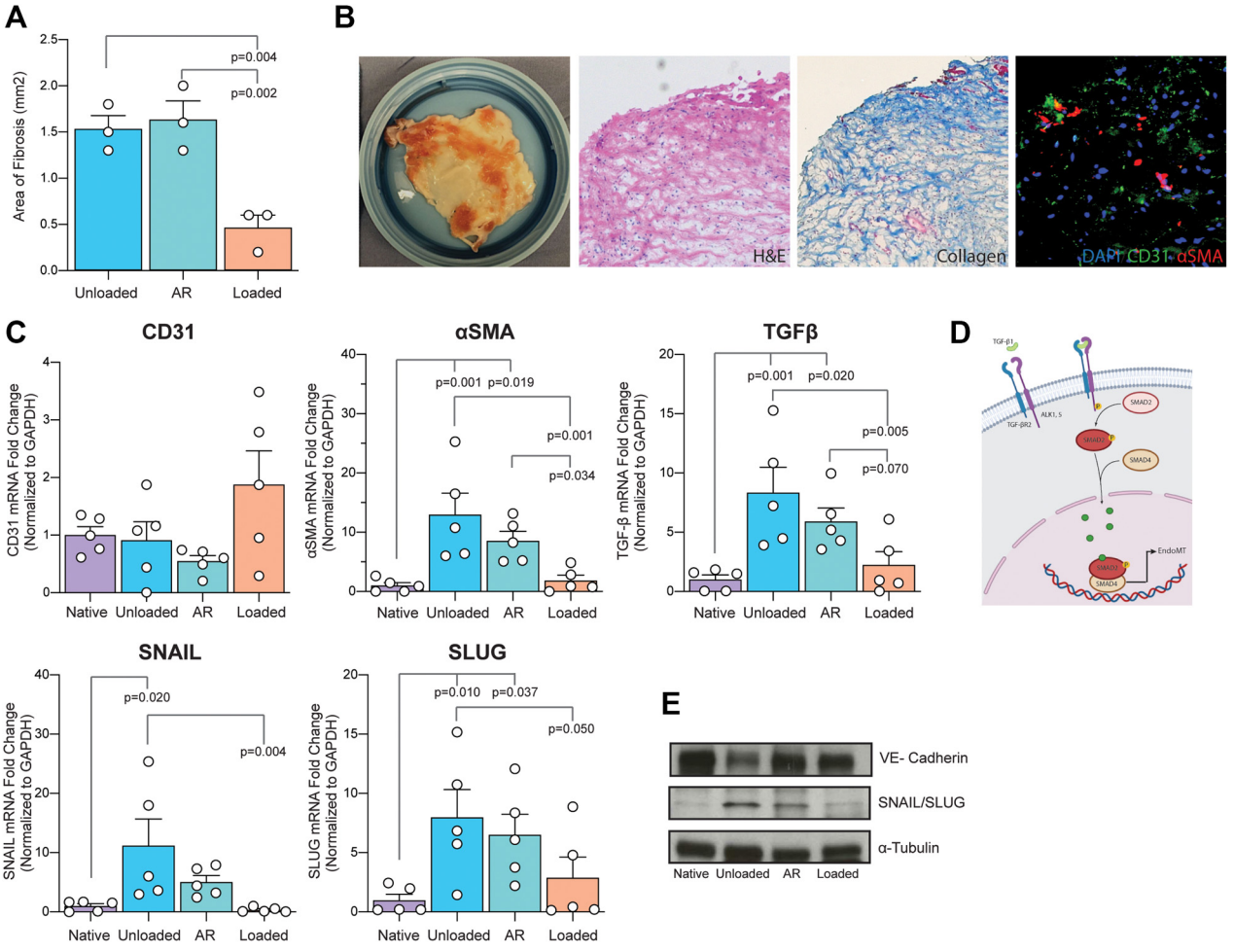

(A) Area of fibrosis in unloaded and regurgitant flow groups is found to be statistically increased compared to the loaded groups. **(B)** EFE tissue from human patient is surgically removed. H&E, Masson trichrome, and immunofluorescence staining with DAPI **(blue),** CD31 **(green),** and αSMA **(red)** show increased fibrosis and endothelial-to-mesenchymal transition (EndoMT). **(C)** Real-time quantitative polymerase chain reaction (RT qPCR) data show increased EndoMT mRNA (αSMA, TGFβ1, SNAIL, and SLUG) in unloaded and aortic regurgitation (AR) groups when compared to loaded and native hearts. **(D)** Schema of the TGFβ pathway shows SMAD cascade activation and upregulation of genes associated with EndoMT. **(E)** Western blot analysis shows increased SNAIL/SLUG protein in unloaded and AR groups when compared to loaded and native groups. GAPDH = glyceraldehyde 3-phosphate dehydrogenase; TGF = transforming growth factor; VE = vascular endothelial; other abbreviations as in Figure 1.

as native hearts. Similarly, we examined EndoMT-specific transcription factor, SNAIL, and found that static and regurgitant flow groups had increased expression of SNAIL (Figure 2C). Another transcription factor, SLUG, was also increased in static and regurgitant flow groups. Because EndoMT occurs through different signaling pathways, we sought evidence by qPCR for whether TGF-β/bone morphogenetic protein pathway plays a role in flow-mediated EndoMT (Figure 2D). We found that static and regurgitant flow groups had significantly increased expression of TGF-β1 (Figure 2C). On the other hand, the normal flow group expressed decreased mRNA expression of TGF-β1 when compared to both static and regurgitant flow groups, but similar levels to the native hearts (Figure 2C). Collectively, these results are congruent with our histologic analysis, providing further evidence that EndoMT in endocardium can be triggered by abnormal flow conditions. We also provide evidence that TGF-β may play a role in flow-mediated EndoMT, as it is increased in static and regurgitant flow groups.

FIGURE 3 **Treatment of Neonatal Transplanted Heart With Losartan Decreases EndoMT and Ameliorates EFE**

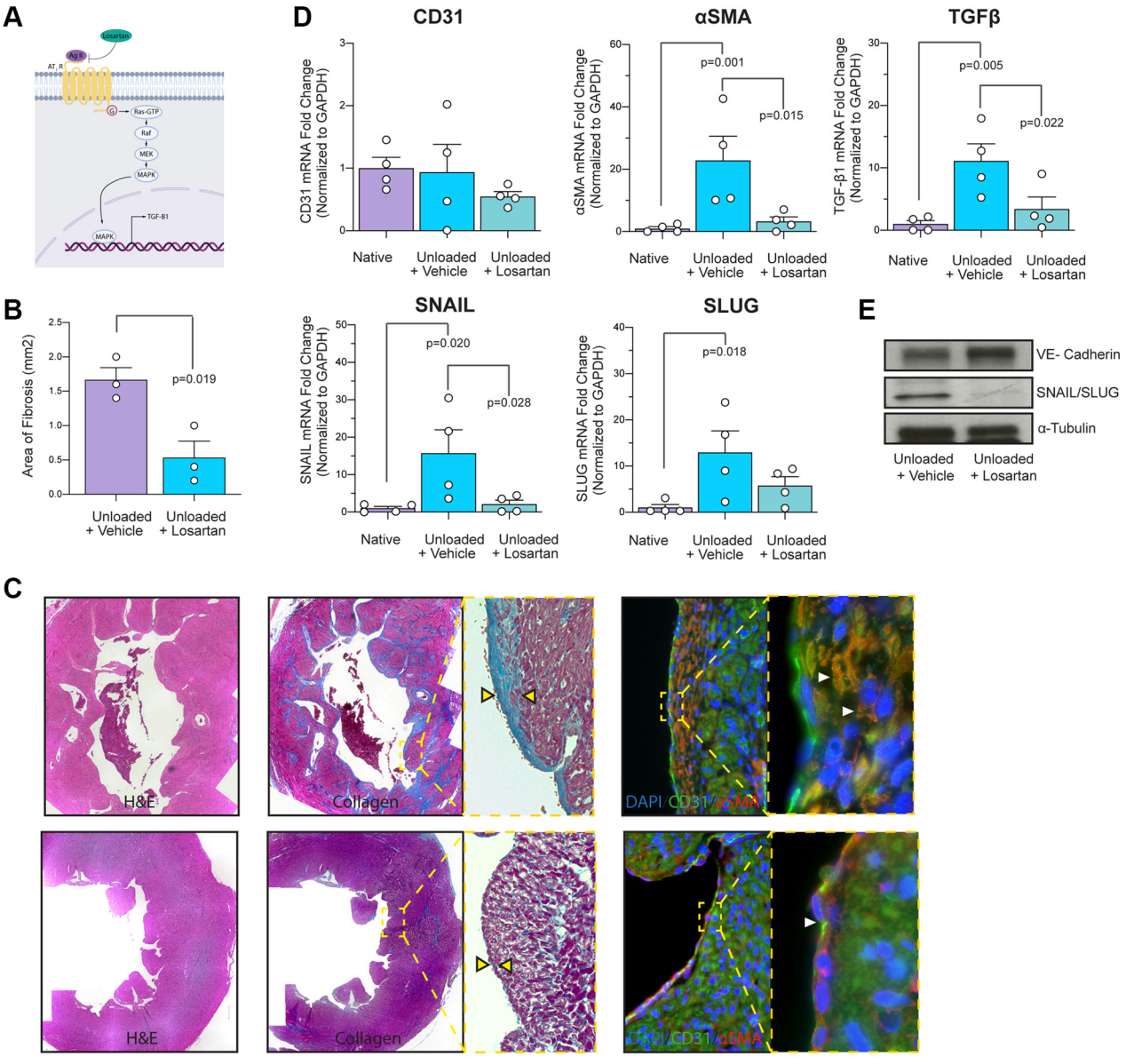

(A) Schema of losartan action on TGFβ production. **(B)** Area of fibrosis measurements shows statistically decreased fibrosis with losartan treatment. **(C)** H&E, Masson trichrome, and immunofluorescence staining with DAPI **(blue),** CD31 **(green),** αSMA **(red),** staining shows decreased endocardial fibroelastosis and EndoMT with losartan treatment. **(D)** RT qPCR shows decreased mRNA associated with EndoMT (α-SMA, TGF-β1, SNAIL, and SLUG) in the unloaded heart with losartan treatment. **(E)** Western blot analysis shows decreased SNAIL/SLUG protein in losartan treated groups denoting decreased EndoMT. Abbreviations as in Figures 1 and 2.

We sought to further validate our findings with corresponding changes in protein expression. To this end, we performed a Western blot assay on extracted proteins from dissected endocardial layer of transplanted hearts with different flow profiles. The static group was found to have higher protein levels of SNAIL/SLUG, and lower level of endothelial marker vascular endothelial (VE)-cadherin. Similarly, the regurgitant flow group also had increased SNAIL/SLUG protein levels but not as high as the static group. VE-cadherin was also decreased in this group. Interestingly, the normal flow group had lower level of SNAIL/SLUG, similar to that of the native heart, and higher expression of VE-cadherin (Figure 2E). Our

FIGURE 4 Examining HUEECs Isolated From LV in Response to Different Flow Conditions

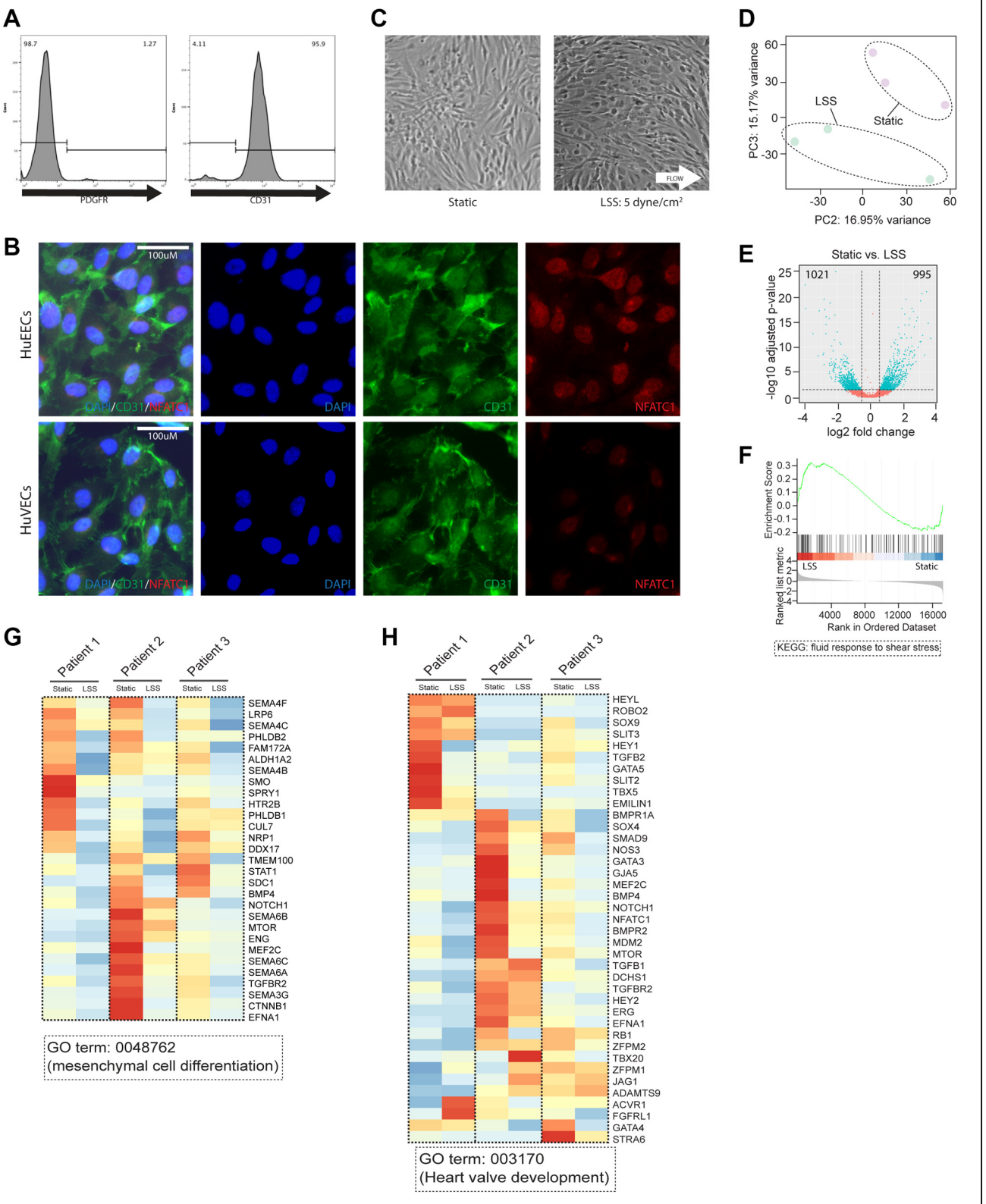

Continued on the next page

results above further confirmed the progression of EndoMT in response to different flow conditions at the protein level.

TREATMENT OF NEONATAL TRANSPLANTED HEART WITH LOSARTAN AMELIORATES ENDOCARDIAL FIBROELASTOSIS. Previous studies have consistently shown the ability of angiotensin II receptor blockers, such as losartan, to decrease fibrosis in the various organ systems (23-26). Losartan is a readily available and medically approved angiotensin II receptor blocker that has been shown to affect TGFβ1 production (**Figure 3A**) and decrease TGFβ-mediated fibrosis (26,27). However, losartan has never been tested in treating EFE. To this effect, we sought to understand the effects of losartan on EFE development using our neonatal heart transplantation model. Based on dosages found in existing literature for treating fibrosis in rodents (n = 4), we treated our static group with losartan (40 mg/kg/day) for 7 days (23,24). Histologic analysis after 7 days of treatment showed that losartan significantly decreased fibrosis area in LV endocardium when compared to the vehicle-treated control group (**Figure 3B**). Immunofluorescence staining also showed that the losartan-treated group had significantly less α-SMA expression compared to the control group, whereas CD31 levels were unchanged (**Figure 3C**).

Next, we sought evidence of corresponding changes in the mRNA and protein expression. We found that the mRNA expression of αSMA was significantly decreased, along with TGF-β1 in the losartan-treated group (**Figure 3D**). Further, we found that the mRNA expression of SNAIL was also significantly decreased (**Figure 3D**). Using Western blot assay to evaluate protein expression, we found that the losartan treatment group showed increased VE-cadherin protein and decreased SNAIL/SLUG protein when compared to the control group (**Figure 3E**). Our results show that losartan treatment can effectively inhibit the development of EFE through interfering with EndoMT.

EXAMINING HUEECs ISOLATED FROM LV IN RESPONSE TO DIFFERENT FLOW CONDITIONS. With our animal models providing evidence of increased EndoMT and EFE progression in hearts with abnormal blood flows, we sought to translate these findings to human endocardium, which has never been studied before in this context. To this end, we obtained discarded endocardial tissue from human patients and isolated HUEECs. Because current literature suggests that endothelial cell origin may dictate cell behavior, we looked for confirmation on the endocardial identity of the isolated cells (28-31). Specifically, we hoped to isolate a CD31-positive population expressing the endocardial specific marker, NFATC1 (32). Using flow cytometry, we show that our HUEEC from all 3 individual patient samples consisted of cells with a high CD31 positivity (>95%), and a low PDGFRβ positivity (<2%) (**Figure 4A**). Using immunofluorescent staining, both strong CD31 surface staining and strong NFATC1 nuclei signaling were observed in HUEECs when compared to HUVECs (**Figure 4B**). These above results showed that HUEECs can be successfully isolated and cultured for in vitro human endocardium modeling.

Several lines of evidence have shown that vascular wall endothelial cells differentially respond to distinct types of shear stress (30,31). However, no studies have been performed on the response of HUEEC to shear stress. After confirming the endocardial lineage identity of the cell isolates, we sought to understand the effects of mechanical forces on HUEECs. Although shear stress calculations have been performed in the adult LV using computational techniques, these values cannot be translated to the pediatric LV (33). Therefore, our team reached a consensus to use an LSS of 5 dyne/cm^2 because it is the peak shear stress experienced in the adult LV during systole and could be considered an acceptable starting point until a validated waveform from a pediatric LV can be calculated in the future.

To apply accurate shear stress on the HUEECs, we used a previously described cone-plate viscometer

FIGURE 4 Continued

Fluorescence-activated cell sorting (FACS) analysis shows high levels of CD31 and low levels of PDGFR in isolated human endocardial endothelial cells (HUEECs). **(B)** Immunofluorescence staining shows increased expression of endocardial-specific marker NFATC1 in HUEECs when compared to human umbilical vein endothelial cells (HUVECs). **(C)** Monolayer of HUEECs under 5 dyne/cm^2 shear stress shows cobblestone architecture and more arrangement in the direction of flow. **(D)** Measurement of cellular orientation angles shows that HUEECs subjected to laminar shear stress (LSS) have a narrow range of angles that align with flow, whereas HUEECs under static conditions have a wide range of angles consistent with disorientation. **(E)** Principle component analysis shows that samples cluster together by application of static or LSS conditions on PC3. **(F)** Volcano plot shows differential expressed genes enriched in static or LSS samples **(G)** Gene set enrichment analysis shows that Kyoto Encyclopedia of Genes and Genomes (KEGG) pathways of fluid response to shear stress are enriched in LSS compared to static groups. Heatmaps show increased gene expression in LSS condition for gene ontology term for **(H)** mesenchymal cell differentiation and (I) heart valve development. PDGFR = platelet-derived growth factor receptor; other abbreviations as in **Figure 1**.

FIGURE 5 Notch Signaling Pathway is Related to Flow-Triggered EFE Remodeling

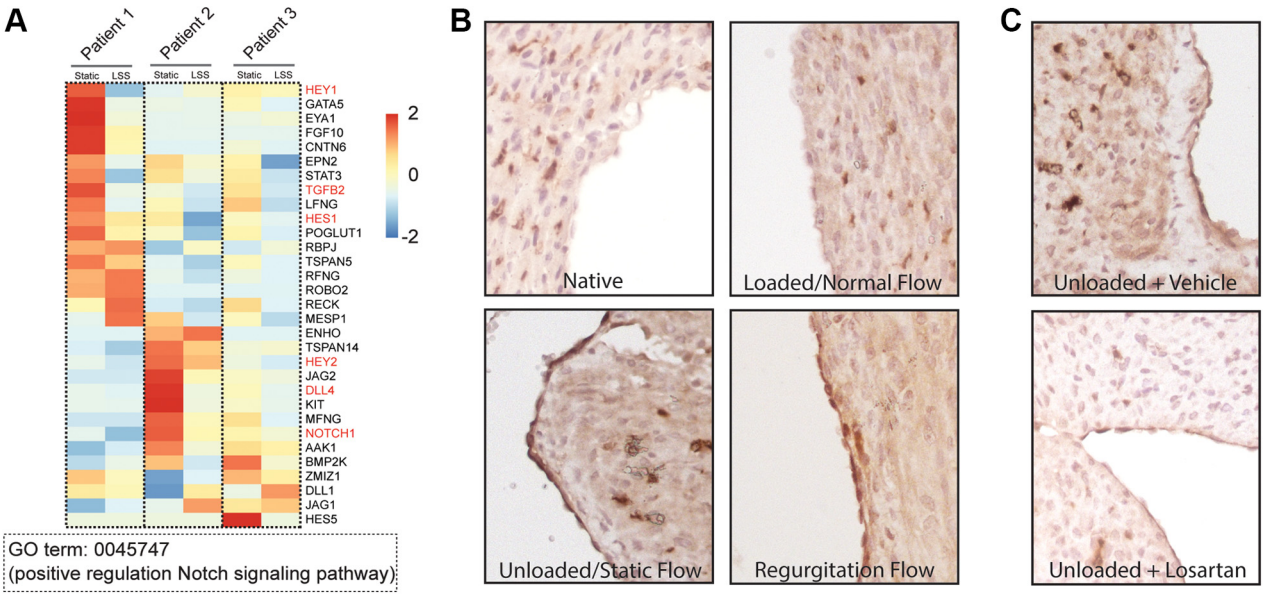

(A) RNA sequence analysis of HUEECs show increase NOTCH1 signaling with static conditions versus LSS. **(B)** NOTCH1 staining in the native, loaded, unloaded, and regurgitant flow models show increased NOTCH1 staining with unloaded/static flow and regurgitant flow groups. **(C)** NOTCH1 staining is found to be decreased with losartan treatment. **(D)** Western blot staining shows increased NOTCH1 protein expression in unloaded and AR samples, consistent with NOTCH1 staining. Similarly, losartan treatment decreases NOTCH1 expression. Abbreviations as in **Figures 1, 2, and 4**.

called the DFS (14). Once the HUEECs were plated on the DFS plate, they were maintained under static (no flow) or exposed to LSS (5 dyne/cm^2) for 24 hours. Microscopic examination of these cells after 24-hour shear stress showed that the HUEEC cell morphology under static conditions had a more disorganized arrangement, whereas HUEECs exposed to LSS were more organized by flow direction and cobblestoned (**Figure 4C**). Measurement of cellular orientation angle shows that the static conditions have a more disorganized orientation as evidenced by a wide range of angles, whereas LSS aligns cells, shown by a narrow range of orientation angles (**Figure 4D**). These results showed that HUEECs uniquely respond to LSS when compared to static conditions. In our analysis, we decided to use biological repeats to discover whether our results would be sustained under different set of biological variables.

RNAseq ANALYSIS OF HUEEC IN RESPONSE TO STATIC AND LSS FLOW CONDITIONS. Using the HUEECs exposed to static and LSS conditions, we performed an RNAseq analysis to understand the effects of these different conditions on human endocardium at the global transcriptome level. Principal component analyses revealed that samples clustered together by application of static or LSS conditions on PC3, whereas PC1 mainly reflected the variation by patient origin of the samples (**Figure 4E,** Supplemental Figure 2A). Pairwise correlation comparison also showed the samples with the same patient origin were clustered together (Supplemental Figure 2B). Differential expressed genes enriched in static (1,021 genes) or LSS (995 genes) conditioned samples were exhibited by volcano plot and heatmap (**Figure 4F,** Supplemental Figure 2C). To confirm that HUEECs responded to shear stress, we performed Gene Set Enrichment Analysis which showed that KEGG pathway of fluid response to shear stress was considerably enriched in LSS samples as compared to static samples (**Figure 4G**).

EndoMT occurs physiologically in the heart during heart valve development through various signaling pathways, but occurs aberrantly during EFE development. To understand whether the different wall shear stresses modulate EFE- or EndoMT-related changes in HUEECs, we analyzed selected gene ontology (GO) terms in our RNA-Seq data (Supplemental Figure 3). Between samples from the same patient, we find that exposure to LSS results in

the suppression of genes associated with mesenchymal cell differentiation (GO term: 0048762) compared to static (no flow conditions) (**Figure 4H**). Additionally, genes typically expressed during heart valve development (GO term: 003170) were also found to be increased in static samples compared to LSS samples (**Figure 4I**). These results indicated that the absence of normal flow in the static condition group induced EndoMT-related gene expression changes. In addition, genes related to the negative regulation of apoptosis pathway (GO term: 2001234) were induced by LSS compared to static samples (Supplemental Figure 2D). Interestingly, not exactly all the same genes changed across HUEECs from different patients which suggested certain individual specific factors regulate EndoMT in response to the lack of normal flow.

We further investigated different potential signaling pathways regulating EndoMT and found that genes associated with activation of the Notch signaling pathway (GO term: 0045747, Hey1, Hey2, and Hes1) were expressed under static (no flow) conditions and suppressed under LSS (**Figure 5A**). Collectively, our RNAseq results showed static (no flow) conditions, similar to the static condition in animal model, trigger EFE and EndoMT-related changes.

To validate the observations derived from the RNAseq experiments, we confirmed the suppression of the same panel of Notch-related genes using real-time qPCR. We further investigated the activation of Notch signaling in the animal model of EFE. Histologic analysis using an antibody against the activated form of Notch1 revealed increased staining on the endocardium in static and regurgitant flow conditions when compared to normal flow and native conditions (**Figure 5B**), thus validating in vitro data. Interestingly, we performed the same analysis in the losartan-treated group, and showed that Notch1 activation decreases with losartan treatment when compared to the control group (**Figure 5C**). Using Western blot, we showed increased protein expression of Notch1 in our static and regurgitant flow conditions. Further, we show that losartan treatment decreases Notch1 expression (**Figure 5D**). Together, these results indicated that both Notch and TGFβ may play a role in flow-mediated EndoMT and EFE development.

DISCUSSION

HLHS is a congenital heart disease defined by a hypoplastic LV and a spectrum of stenosis or atresia of the associated mitral and aortic valves (1). The high morbidity and mortality associated with this disease process is often complicated by the presence of EFE, which disrupts the systolic and diastolic function of the LV. Clinical research has consistently shown the increased risk of complications and death when EFE is present in HLHS (3,34). Thus, this study was designed to address 2 areas of interest: the triggers of EFE development (namely, the absence of normal flow), and potential therapies to ameliorate EFE formation.

Previous work has used neonatal heterotopic heart transplantation in rodents to study EFE development (20,21). Although flow dynamics in the LV, absence of flow, and LV distension have all been postulated as triggers for EFE development in this model, solid evidence has not been substantiated (12). However, in patients, EFE is strongly associated with flow disturbances, and often recurs in situations where abnormal flow persists, emphasizing the importance of the flow patterns in our experiments (9); thus the objective of our research is to investigate EFE development in the context of both static and disturbed/regurgitant flow.

Previously, Xu et al (6) showed that human EFE tissue had increased mRNA expression of αSMA, SNAIL, and SLUG compared to healthy human LV tissue, suggesting that EndoMT may be a player in EFE development. Further support is substantiated by histologic evidence showing coexpression of mesenchymal and endothelial markers in pathologic samples of human EFE. Interestingly, lineage tracing studies in mice by Zhang et al (10) have suggested that EFE development is attributed more to epicardial-to-mesenchymal transition rather than EndoMT. Clearly, EFE development is a complex mechanism affected by different physical processes, particularly when extrinsic factors such as flow, genetics, and epigenetics are at play, and require further investigation.

In this context, we set up 3 groups of neonatal heart transplantation, each group experiencing different types of flow in the LV, namely, severely limited flow (static), regurgitant/turbulent flow, and normal flow. We provide evidence that the absence of normal flow promotes EFE development, as both static and regurgitant flow groups developed significant fibrosis and increased EndoMT markers. Evidence of abnormal flow promoting EndoMT in VE has been well recognized, but its effects in the endocardium have been less studied. In the context of clinical findings highlighting the association between disturbed flow and EFE, our data strengthens the hypothesis that abnormal flow promotes fibrosis in the endocardium through EndoMT. This new

knowledge may be therapeutically important in cases of recurrent EFE in that normal flow should be reconstituted whenever feasible.

EndoMT occurs through different pathways, such as the TGF-β/bone morphogenetic protein pathway, NOTCH pathway, and Wnt-catenin pathway (22). In EFE tissue found in patients, EndoMT is thought to occur largely through activation of the TGFβ pathway (6). Similarly, in this study, we show in our model that the lack of normal flow (static and regurgitant flow groups) increased TGFβ expression, suggesting that this pathway plays a role in EFE formation in flow-mediated EndoMT. This process is likely similar across cardiovascular endothelium as examples of TGFβ-mediated EndoMT can be found in HUVECs experiencing abnormal flow (15,17,29). Interestingly, a recent study used murine heterotopic heart transplantation and murine lineage-tracing studies to suggest that EFE formation occurs through epicardial-to-mesenchymal transition more so than EndoMT (10). Our rodent model, although limited by the lack of lineage-tracing species, has the advantage of simulating multiple flow profiles (namely, aortic regurgitation) such as those observed in human patients. Although our study suggests that EndoMT is a significant process in EFE development attributed to multiple disturbed flow profiles, we do not exclude the role of epicardial-to-mesenchymal transition. Rather, our study confirms that EFE development is a complex process affected by various factors and that 1 mechanism may not be mutually exclusive of the other.

Clinical studies show that EFE is a risk factor for poor outcomes, especially considering that treatment modalities are few and far between (4,5). Current therapies are mainly surgical and, in some cases, the EFE can recur even after resection. Literature provides examples of losartan, an angiotensin II type 1 receptor antagonist, conferring benefit in decreasing fibrotic processes in peripheral vasculature by decreasing TGFβ production (23,24,27,35). Clinically, losartan is used to treat heart failure and prevent cardiac remodeling (36). Thus, we sought the novel application of this clinically available drug in abrogating EFE development in our animal model. After 7 days of systemic delivery, we documented a significant decrease in the extent of fibrosis and EndoMT. Although this suggests that losartan is effective in abrogating EFE, the mechanism can be multifold and through various pathways. A large body of evidence suggests that losartan works predominantly by inhibiting the TGF-β pathway, but other studies indicate that angiotensin II type 1 can also affect Wnt/B-catenin and Notch pathways. Our animal study shows decreased Notch1 activity in losartan-treated groups, suggesting the inhibition of other signaling cascades to limit EndoMT and subsequent EFE development. Although further studies must be performed, this finding is highly significant as medical treatments do not exist for EFE and the novel application of this readily available drug can potentially limit EFE formation and promote better clinical outcomes.

Another particularly interesting EndoMT pathway is the Notch signaling pathway, as it plays a complex role in normal and abnormal heart development. Notch signaling is highly conserved in the endocardium, and is essential in physiologic EndoMT during cardiac development, as it has been shown to regulate valve formation and morphogenesis (32). On the other hand, studies have documented germline mutations in Notch1 signaling in patients with a family history of HLHS, as well as epigenetic changes in Notch1 in HLHS-derived induced pluripotent stem cells (11,13,14,37). One surprising result from our data is that exposure of HUEECs to LSS results in a decrease in Notch1 activity. Moreover, we find evidence in our animal experiments that static and regurgitant flow groups had increased activated Notch1 protein in the endocardium, further suggesting that Notch may also play a role in flow-mediated EFE development. Additionally, previous reports have shown that exposing HUVECs to LSS results in the activation of Notch, whereas we show decreased Notch activity in HUEECs exposed to LSS. Taken together, these data suggest that modulation of flow-mediated activation of Notch signaling is distinct in endocardial versus vascular endothelial cells. Understanding how the Notch pathway further interplays with TGF-β pathway and EndoMT in EFE tissue will be a major focus of our future research.

The response of HUVECs to various types of flow has been well studied. As more is being discovered on endothelial behavior, these studies emphasize the ability of endothelial cells from different locations to behave differently based on the flow applied (18,28-31,38) . Surprisingly, research on the influence of flow on human endocardium remains relatively sparse. Given that our data suggest that the absence of laminar flow can trigger EndoMT in rodent endocardium, we sought to determine whether these effects are also observed in human endocardium. To this end, we isolated HUEECs from human LV tissue and exposed them to shear stresses in vitro for 24 hours. Recent advances in imaging modalities have been able to calculate shear stresses in large tubular vessels and in adult LVs, but the exact shear stresses in the pediatric LV have not been elucidated. Thus,

we believed that an LSS of 5 dyne/cm^2 was an acceptable starting point given its correlation with peak systolic wall shear stress (WSS) in the adult heart. Still, our group is actively researching the complex WSS in the pediatric LV, which will provide more accurate flow profiles for our future testing.

Following flow experiments, our RNAseq analyses show that HUEECs are able to sense and respond to LSS. Further, our analyses show that the presence of LSS decreased expression of genes associated with heart valve development, which occurs through EndoMT and mesenchymal differentiation. Although our data are limited by the genetic variations between patients, transcriptome changes resulting from static and LSS conditions on HUEECs from the same patient emphasize our findings. Our results validate our hypothesis that flow plays an integral role in homeostasis at the endocardial level in human. More specifically, change in flow conditions may push endocardial endothelial cells into a more mesenchymal phenotype. This may be especially true in cells with increased plasticity, particularly in developing pediatric patients. Interestingly, we did not detect any significant differences in gene expression for the TGFβ pathway, which is seemingly contradictory to our animal studies. However, a couple of key differences must be emphasized. First, our flow studies were performed on isolated HUEECs without other essential cell types that produce TGF-β, such as cardiomyocytes and cardiac fibroblasts or with treatment with TGF-β. The focus of our initial studies was to show that flow can affect HUEECs into mesenchymal cell differentiation. Secondly, human endothelial cells can discriminate between a range of flow profiles. Thus, the focus of our future research will be to better understand this dynamic between HUEECs and other cardiac-resident cell types by using multiple cell types in our flow experiments, and to further refine the applied flow profiles. Nevertheless, the changes in HUEEC gene expression in response to various WSS are novel and will be another active area of our future research.

STUDY LIMITATIONS. First, in the regurgitant flow group, the regurgitant flow tends to distend the LV. Distension of the LV has been described clinically and in research to contribute to cardiac dysfunction and fibrosis (21). However, although ventricular distension should be considered a factor, literature also suggests that flow promotes fibrosis in the cardiovascular system, similar to our results, and its influence should not be considered insignificant. Second, the normal flow model does not have the same preload as a normal heart and the oxygenation of the blood is likely mixed. Echocardiographic verification indicates that flow does occur in the LV and our analysis suggests that despite these limitations, the normal flow heart has very limited EFE and EndoMT. Another consideration is the origin of our HUEECs, in that they are isolated from a normal LV of patients undergoing surgical treatment for existing congenital heart abnormalities. These pathologies play a role in endothelial behavior, as many are associated with genetic mutations, which may explain different sets of genes related to EndoMT are activated in HUEECs from different patients. To limit these confounders, we compared static and LSS within patients.

CONCLUSIONS

Future studies should be geared towards isolating HUEECs from healthy LV tissue, although this task may be difficult given the invasiveness. We recognize that this in vitro cell model is simplified and does not account for the interaction with cardiomyocytes, fibroblasts, and other cell types present in the developing heart. Future studies will seek to understand these interactions using 3-dimensional co-culture or organoid models in the context of different flow conditions.

This study shows the pathologic effect of abnormal flow on the endocardium for the first time. Using an animal model of EFE with different flow settings, our results emphasize abnormal flow promoting EFE development through the EndoMT which were mediated by TGF-β and Notch pathways. More importantly, we translate our findings in animal model to human-derived cells. Shear stress experiments on human endocardial cells indicate, for the first time, that HUEECs respond to biomechanical stimulation and that the lack of flow promotes certain genes associated with mesenchymal differentiation. Furthermore, we propose losartan as a novel potential therapy for EFE as it is able to abrogate EFE development in our animal model.

FUNDING SUPPORT AND AUTHOR DISCLOSURES

This work has been supported by Boston Children's Hospital, Department of Cardiovascular Surgery, Internal Funding Boston Children's Hospital, Kaplan Fellowship. The authors have reported that they have no relationships relevant to the contents of this paper to disclose.

ADDRESS FOR CORRESPONDENCE: Dr Nicholas A. Oh, Department of Cardiovascular Surgery, Cleveland Clinic Foundation, 9500 Euclid Avenue, J4-133, Cleveland, Ohio 44195, USA. E-mail: Ohn2@ccf.org.

PERSPECTIVES

COMPETENCY IN MEDICAL EDUCATION: Clinical studies show that the presence of EFE in children with congenital heart disease contributes to increased morbidity and mortality. Understanding the triggers of EFE formation will be impactful in treating this disease. This study shows for the first time that endocardial endothelial cells are affected by various flow conditions, and that abnormal flow promotes EFE formation, at least in part through EndoMT. Further, losartan treatment is shown for the first time to ameliorate EFE progression.

TRANSLATIONAL OUTLOOK: This study shows a correlation between abnormal flow and EFE formation, and that losartan treatment may ameliorate the severity of EFE. Thus, it is important to consider addressing abnormal flow in children with EFE and the potential of losartan in abrogating EFE severity.

REFERENCES

1. McElhinney DB, Vogel M, Benson CB, et al. Assessment of left ventricular endocardial fibroelastosis in fetuses with aortic stenosis and evolving hypoplastic left heart syndrome. *Am J Cardiol*. 2010;106:1792-1797.

2. Herrin MA, Zurakowski D, Baird CW, et al. Hemodynamic parameters predict adverse outcomes following biventricular conversion with single-ventricle palliation takedown. *J Thorac Cardiovasc Surg*. 2017;154:572-582.

3. Emani SM, McElhinney DB, Tworetzky W, et al. Staged left ventricular recruitment after single-ventricle palliation in patients with borderline left heart hypoplasia. *J Am Coll Cardiol*. 2012;60:1966-1974.

4. Emani SM, Bacha EA, Mcelhinney DB, et al. Primary LV rehabilitation is effective in maintaining two-ventricle physiology in the borderline left heart. *J Thorac Cardiovasc Surg*. 2010;138:1276-1282.

5. Freud LR, Mcelhinney DB, Marshall AC, et al. Fetal aortic valvuloplasty for evolving hypoplastic left heart syndrome: postnatal outcomes of the first 100 patients. *Circulation*. 2015;130:638-645.

6. Xu X, Friehs I, Hu TZ, et al. Endocardial fibroelastosis is caused by aberrant endothelial to mesenchymal transition. *Circ Res*. 2015;116:857-866.

7. Li Y, Lui KO, Zhou B. Reassessing endothelial-to-mesenchymal transition in cardiovascular diseases. *Nat Rev Cardiol*. 2018;15:445-456.

8. Pesevski Z, Kvasilova A, Stopkova T, et al. Endocardial fibroelastosis is secondary to hemodynamic alterations in the chick embryonic model of hypoplastic left heart syndrome. *Dev Dyn*. 2018;247:509-520.

9. Weixler V, Marx GR, Hammer PE, Emani SM, del Nido PJ, Friehs I. Flow disturbances and the development of endocardial fibroelastosis. *J Thorac Cardiovasc Surg*. 2020;159:637-646.

10. Zhang H, Huang X, Liu K, et al. Fibroblasts in an endocardial fibroelastosis disease model mainly originate from mesenchymal derivatives of epicardium. *Cell Res*. 2017;27:1157-1177.

11. Durbin MD, Cadar AG, Williams CH, et al. Hypoplastic left heart syndrome sequencing reveals a novel NOTCH1 mutation in a family with single ventricle defects. *Pediatr Cardiol*. 2017;38:1232-1240.

12. Lurie PR. Changing concepts of endocardial fibroelastosis. *Cardiol Young*. 2010;20:115-123.

13. Hinton RB, Martin LJ, Tabangin ME, Mazwi ML, Cripe LH, Benson DW. Hypoplastic left heart syndrome is heritable. *J Am Coll Cardiol*. 2007;50:1590-1595.

14. Kelle AM, Qureshi MY, Olson TM, Eidem BW, O'Leary PW. Familial incidence of cardiovascular malformations in hypoplastic left heart syndrome. *Am J Cardiol*. 2015;116:1762-1766.

15. Blackman BR, García-Cardeña G, Gimbrone MA. A new in vitro model to evaluate differential responses of endothelial cells to simulated arterial shear stress waveforms. *J Biomech Eng*. 2002;124:397-407.

16. Koefoed K, Veland IR, Pedersen LB, Larsen LA, Christensen ST. Cilia and coordination of signaling networks during heart development. *Organogenesis*. 2014;10:108-125.

17. DePaola N, Gimbrone MA, Davies PF, Dewey CF. Vascular endothelium responds to fluid shear stress gradients. *Arterioscler Thromb*. 1992;12:1254-1257.

18. DeStefano JG, Williams A, Wnorowski A, Yimam N, Searson PC, Wong AD. Real-time quantification of endothelial response to shear stress and vascular modulators. *Integr Biol*. 2017;9(4):362-374.

19. Moonen JRAJ, Lee ES, Schmidt M, et al. Endothelial-to-mesenchymal transition contributes to fibro-proliferative vascular disease and is modulated by fluid shear stress. *Cardiovasc Res*. 2015;108:377-386.

20. Friehs I, Illigens B, Melnychenko I, Zhong-Hu T, Zeisberg E, Del Nido PJ. An animal model of endocardial fibroelastosis. *J Surg Res*. 2013;182:94-100.

21. Shimada S, Del Nido PJ, Friehs I. Development of a vascularized heterotopic neonatal rat heart transplantation model. *Eur Surg Res*. 2016;57(3-4):240-251.

22. Kovacic JC, Mercader N, Torres M, Boehm M, Fuster V. Epithelial-to-mesenchymal and endothelial-to-mesenchymal transition: from cardiovascular development to disease. *Circulation*. 2012;125:1795-1808.

23. Molina-Molina M, Serrano-Mollar A, Bulbena O, et al. Losartan attenuates bleomycin induced lung fibrosis by increasing prostaglandin E2 synthesis. *Thorax*. 2006;61:604-610.

24. Gay-Jordi G, Guash E, Benito B, et al. Losartan prevents heart fibrosis induced by long-term intensive exercise in an animal model. *PLoS One*. 2013;8:1-8.

25. Croquet V, Moal F, Veal N, et al. Hemodynamic and antifibrotic effects of losartan in rats with liver fibrosis and/or portal hypertension. *J Hepatol*. 2002;37:773-780.

26. Yao Y, Li Y, Zeng X, Ye Z, Li X, Zhang L. Losartan alleviates renal fibrosis and inhibits endothelial-to-mesenchymal transition (EMT) under high-fat diet-induced hyperglycemia. *Front Pharmacol*. 2018;9:1-12.

27. Wu M, Peng Z, Zu C, et al. Losartan attenuates myocardial endothelial-to-mesenchymal transition in spontaneous hypertensive rats via inhibiting TGF-β/Smad signaling. *PLoS One*. 2016;11:1-13.

28. Zhou J, Li YS, Chien S. Shear stress-initiated signaling and its regulation of endothelial function. *Arterioscler Thromb Vasc Biol*. 2014;34:2191-2198.

29. Davies PF. Hemodynamic shear stress and the endothelium in cardiovascular Pathophysiology. *Nat Clin Pract Cardiovasc Med*. 2009;6:16-26.

30. García-Cardeña G, Comander J, Blackman B, Anderson K, Gimbrone M. Mechanosensitive endothelial gene expression profiles: scripts for the role of hemodynamics in atherogenesis? *Ann N Y Acad Sci*. 2001;947:1-6.

31. Hong D, Jaron D, Buerk DG, Barbee KA. Heterogeneous response of microvascular endothelial cells to shear stress. *Am J Physiol Hear Circ Physiol*. 2006;290:2498-2508.

32. Wu B, Wang Y, Lui W, et al. Nfatc1 coordinates valve endocardial cell lineage development required for heart valve formation. *Circ Res*. 2011;23:1–7.

33. McCormick ME, Manduchi E, Witschey WRT, et al. Integrated regional cardiac hemodynamic imaging and RNA sequencing reveal corresponding heterogeneity of ventricular wall shear stress and endocardial transcriptome. *J Am Heart Assoc*. 2016;5:e003170.

34. Feinstein JA, Benson DW, Dubin AM, et al. Hypoplastic left heart syndrome: current considerations and expectations. *J Am Coll Cardiol*. 2012;59(suppl 1):S1–S42.

35. Bartko PE, Dal-Bianco JP, Guerrero JL, et al. Effect of losartan on mitral valve changes after myocardial infarction. *J Am Coll Cardiol*. 2017;70:1232–1244.

36. Pitt B, Poole-wilson PA, Segal R, et al. ELITE II — effect of losartan compared with captopril on mortality in patients with symptomatic heart failure. *Lancet*. 2000;355:1582–1587.

37. Miao Y, Tian L, Martin M, et al. Intrinsic endocardial defects contribute to hypoplastic left heart syndrome. *Cell Stem Cell*. 2020;27:574–589.e8.

38. James BD, Allen JB. Vascular endothelial cell behavior in complex mechanical microenvironments. *ACS Biomater Sci Eng*. 2018;4:3818–3842.

KEY WORDS congenital heart disease, endocardial endothelial cells, endocardial fibroelastosis, endothelial-to-mesenchymal transition, wall shear stress

APPENDIX For an expanded Methods section as well as supplemental figures and tables, please see the online version of this paper.